

An Investigation of Tropical Cyclone Development Pathways as an Indicator of Extratropical Transition

Ishan DATT

Department of Applied Physics and Applied Mathematics, Columbia University, New York, USA

Suzana J. CAMARGO

Lamont-Doherty Earth Observatory, Columbia University, New York, USA

Adam H. SOBEL

*Department of Applied Physics and Applied Mathematics and Department of Earth and Environmental Sciences,
Columbia University, New York, USA*

Ron McTAGGART-COWAN

Numerical Weather Prediction Research Section, Environment Canada, Canada

and

Zhuo WANG

Department of Atmospheric Sciences, University of Illinois, Illinois, USA

(Manuscript received 8 September 2021, in final form 25 April 2022)

Abstract

A significant fraction of tropical cyclones develop in baroclinic environments, following tropical cyclogenesis “pathways” that are characterized by dynamical processes often associated with mid-latitudes. This study investigates whether such storms are more likely to undergo subsequent extratropical transition than those that develop in more typical, non-baroclinic environments. We consider tropical cyclones globally in the period of 1979–2011 using best-track datasets and define the genesis pathway of each storm using McTaggart-Cowan’s classification: non-baroclinic, low-level baroclinic, trough-induced, and weak and strong tropical transition. In each basin, we analyze the total number and the fraction of storms that underwent extratropical transition as well as their seasonality and storm tracks according to their genesis pathways. The relationship between the pathways and extratropical transition is statistically significant in the North Atlantic and Western North Pacific, where the strong tropical transition and the trough-induced pathways have a significantly greater extratropical fraction compared with all other pathways, respectively. Latitude, longitude, and environmental factors, such as sea surface temperature and vertical shear, were further analyzed to explore whether storms in these pathways occur in environments conducive to extratropical transition, or whether a “memory” of the genesis pathway persists throughout the storm life cycle. After controlling for genesis latitude, the relationship between the strong tropical transition and trough-

Corresponding author: Suzana J. Camargo, Lamont-Doherty Earth Observatory, Columbia University, P.O. Box 1000, 61 Route 9W, Palisades, NY 10964, USA
E-mail: suzana@ldeo.columbia.edu
J-stage Advance Published Date: 13 May 2022



induced pathways and the extratropical transition occurrence remains statistically significant, implying a lasting effect from the pathway on the probability of an eventual extratropical transition.

Keywords tropical cyclones; extratropical transition; cyclogenesis

Citation Datt, I., S. J. Camargo, A. H. Sobel, R. McTaggart-Cowan, and Z. Wang: An investigation of tropical cyclone development pathways as an indicator of extratropical transition. *J. Meteor. Soc. Japan*, **100**, 707–724, doi:10.2151/jmsj.2022-037.

1. Introduction

Extratropical transition (ET) is the process by which a tropical cyclone transforms into an extratropical cyclone (Evans et al. 2017; Jones et al. 2003; Keller et al. 2019). Hurricane Sandy (2012) is a well-known recent example of a storm that underwent ET. The devastation brought by Sandy was exacerbated by the ET process, as its wind field was significantly enlarged, and baroclinic (i.e., extratropical) processes contributed to its intensification (Galarneau et al. 2013). Storms that undergo ET can also generate hazards further downstream, and in the case of the Atlantic, this could lead to severe impacts in Europe (Sainsbury et al. 2020). Whether a given storm will undergo ET at any given time depends on its internal state and large-scale environment, such that a statistical model based on observable metrics of that internal state and large-scale environment can predict ET with some skill (Bieli et al. 2020). Here, we examine whether the physical pathway by which a storm originally formed influences its probability of undergoing ET.

Tropical cyclogenesis is the process by which a tropical cyclone forms. Studies of tropical cyclogenesis typically focus on the environmental conditions in which genesis occurs, on the dynamical and thermodynamical processes by which it occurs, or both. A recent review of the processes by which a tropical wave develops into a tropical cyclone can be found in the study by Emanuel (2018). Although this tropical development pathway is the dominant one, it is not unique in leading to the formation of tropical cyclones. Mauk and Hobgood (2012) pointed out the dominant role of non-tropical systems in those cases of genesis that occur over cool sea surface temperatures. In many such cases, a strong extratropical precursor evolves into a warm-core tropical cyclone, as first discussed by Davis and Bosart (2003, 2004). Such cases of genesis from baroclinic precursors represent about 16 % of the global tropical cyclones (McTaggart-Cowan et al. 2013).

McTaggart-Cowan et al. (2008, 2013) developed a classification scheme to separate the different genesis pathways, which we will apply here. The five pathways are labelled as non-baroclinic (NB), low-level baroclinic (LLB), trough-induced (TI), strong tropical transition (STT), and weak tropical transition (WTT). The non-baroclinic group can also be described as “traditional tropical development” and constitutes the majority of tropical cyclones globally. Non-baroclinic storms form in environments with weak upper-level synoptic quasigeostrophic forcing for ascent and minimal lower-level baroclinicity, i.e., the deep tropics and environments similar to it. Non-baroclinic storms develop along one, or a combination of multiple, of the following tropical pathways: mesoscale convective vortex development, hot tower spinup, vortex merger, stability profile modification, and surface flux enhancement (Tang et al. 2020). By contrast, low-level baroclinic storms develop in areas with weak synoptic forcing but strong lower-level baroclinicity. Storms in the trough-induced group form in environments of strong upper-level forcing and very weak low-level baroclinicity. Tropical transition refers to a process during which an asymmetric, cold-core, extratropical cyclone transitions into an axisymmetric, warm-core tropical cyclone (Bentley and Metz 2016). Weak tropical transition storms are initiated under conditions of strong synoptic forcing with medium values of low-level baroclinicity. By contrast, strong tropical transition storms are initiated under conditions of strong synoptic forcing with high values of low-level baroclinicity. Fudeyasu and Yoshida (2018) also considered the environmental conditions associated with different types of genesis in the western North Pacific but used different genesis categorizations from those in the study by McTaggart-Cowan et al. (2008, 2013).

The question we explore here is whether there is a relationship between the genesis pathway by which a storm forms and the likelihood that it will later undergo ET. We analyze genesis pathways, whether a storm undergoes ET, and other storm and environmental

properties to determine whether such a relationship exists. We conduct this analysis separately in the following tropical cyclone basins: North Atlantic, Western North Pacific, Eastern North Pacific, North Indian Ocean, South Indian Ocean, Australian region, and South Pacific.

This study begins with descriptions of the datasets used. Prior studies by Bieli et al. (2019) and McTaggart-Cowan et al. (2013) on the global climatology of ET and development pathways, respectively, have been used in this analysis and are summarized in Section 2. Section 3 presents our results. The study concludes with a summary and implications of our results in Section 4.

2. Data and methods

2.1 Datasets

The tropical cyclone best-track datasets from the National Hurricane Center (North Atlantic and Eastern North Pacific) and the Joint Typhoon Warning Center (Western North Pacific, North Indian Ocean and Southern Hemisphere), with additional information on ET provided by Bieli et al. (2019), are used here. The best-track datasets include all tropical cyclones from the period of 1979–2017 with lifetime maximum wind speed greater than 35 kt. The parameters used from the best-track datasets include basin, as well as date, time, longitude and latitude coordinates, and wind speed for all 6-hourly snapshots throughout the duration of each storm. The boundaries for each basin are listed in Table 1. Additionally, we consider the ET marker and ET date/hour from Bieli et al. (2019). The ET marker is 0 if the storm did not undergo ET or 1 if the storm underwent ET. The classification of a storm as ET or non-ET is based on the cyclone phase space developed by Hart (2003) and modified by Bieli et al. (2019).

Bieli et al. (2019) found that ET fractions substantially vary between the seven different basins with the highest ET fractions occurring in the North Atlantic and Western North Pacific, whereas the North Indian Ocean had the lowest. Furthermore, in the Southern Hemisphere, the ET seasonal cycle varies much less than that in the Northern Hemisphere (Bieli et al. 2019).

The third dataset used for this study was created by McTaggart-Cowan et al. (2013). This dataset contains a classification of tropical storm development pathways for the period of 1948–2011. Storms are classified into the five cyclogenesis pathways discussed earlier (McTaggart-Cowan et al. 2013). To develop this classification scheme, many parameters were ex-

Table 1. Ocean basin definitions.

Basin	Acronym	Longitudes
North Atlantic	NAT	American coast to 30°E
Western North Pacific	WNP	100°E–180°
Eastern North Pacific	ENP	180° to American coast
North Indian Ocean	NI	30–100°E
South Indian Ocean	SI	30–90°E
Australian region	AUS	90–160°E
South Pacific	SP	160°E–120°W

amined for the following three criteria: representation of the synoptic-scale near-storm environment, dynamic significance with respect to the theories of tropical cyclogenesis, and differences in structure, evolution, or intensity for the different types of tropical cyclogenesis identified by theoretical models (McTaggart-Cowan et al. 2008). Based on these criteria, the following two parameters were chosen as the basis for pathway classification: Q , representing mean upper-level quasi-nondivergent Q -vector convergence, and Th , representing lower-level thickness asymmetry. The mean upper-level Q -vector convergence is defined as the average convergence of the 400–200 hPa Q -vector field within a 6° radius of the storm center (McTaggart-Cowan et al. 2008). The lower-level thickness asymmetry is defined as the maximum difference in the mean hemispheric (semicircle) 1000–700-hPa thickness values within 10° of the storm center on the dial plots, normalized by the mean thickness in the same area (McTaggart-Cowan et al. 2008). Each pathway represents a combination of a low, medium, or high metric value of the Q and Th parameters (McTaggart-Cowan et al. 2008). The pathway classification is a unique parameter as only data from the evolution of the near-vortex environment from the 36-hour period leading up to the time of the initial storm report in the best-track record is used to classify the storms (McTaggart-Cowan et al. 2008).

We combined the ET flag from Bieli et al. (2019) and the storm development pathway classification from McTaggart-Cowan et al. (2013) with the best-track datasets. Only the period of 1979–2011 was used in our analysis because this is the common period of all datasets. Currently, the classification of storms by pathway after 2012 is unavailable due to data and script losses of the original files that generated the pathway classification dataset. The resulting combined dataset includes the storm ID, ET marker, and storm development pathway classification, along with all standard best-track dataset parameters.

2.2 *ET fraction statistical analysis*

A statistical analysis was conducted to determine if storms in a given pathway have a higher probability of undergoing ET. We define “ET Fraction” as the number of storms that undergo ET divided by the total number of storms in a sample. Storms were sorted by basin and pathway to compare the ET fraction of all storms in the pathway against the ET fraction of all other storms in the basin.

A Monte Carlo simulation was conducted to determine whether a given pathway’s ET fraction was statistically significantly different from the other pathways in the same basin. The bootstrapping was performed by sampling the probability distributions of ET and non-ET storms. The pathway of interest was not included in the sampling for random draws. One thousand sets of n synthetic storms were randomly generated, where n denotes the number of actual observed storms in the genesis pathway of interest in the given basin. Each synthetic storm was labelled with either a 0 for non-ET or 1 for ET. Values of 1 were assigned randomly but with a probability equal to the ET fraction of the set of storms in the basin that formed via all other genesis pathways other than the one of interest. In each of these 1000 sets, the ET fraction was calculated. By construction, the average of these 1000 synthetic ET fractions will be equal to the ET fraction of the storms in the combined set of all other pathways, but the individual values differ because n is finite (and fairly small in some cases). If a development pathway had an ET fraction greater than the 95th percentile or smaller than the 5th percentile of generated ET fractions, it was determined that the ET fraction of storms in the pathway was statistically significantly distinct from that of the other pathways with a confidence level greater than 95 %. This statistical analysis was conducted for all basins and development pathways.

2.3 *Environmental statistical analysis*

A statistical analysis was conducted on the distributions of latitude, longitude, sea surface temperature and vertical shear to determine the similarity of the environmental conditions in the different pathways. Daily environmental data for winds and sea surface temperature from the ERA-Interim reanalysis at the day and location of the storm genesis and lifetime maximum intensity were analyzed (Dee et al. 2011). The horizontal grid spacing of the ERA-Interim data is approximately 80 km.

The vertical wind shear is defined as the magnitude of the difference between the vector winds at 850 hPa

and 200 hPa. The sea surface temperature and vertical shear values used in the final analysis were calculated by averaging vertical shear and sea surface temperature data within a 500-km radius of the storm. We use the simple area average because we are looking only at the genesis phase of the storm life cycle, when the circulation’s impact on deep-layer shear could reasonably be expected to be quite small.

The distributions of latitude, longitude, sea surface temperature, and vertical shear at the times the storms first reached 35-kt wind speed were examined for all pathways. The environmental variable analysis was also conducted at the point of maximum intensity for all storms. The results from the latter will not be presented here because they were similar to those obtained at genesis.

The distributions were analyzed using boxplots to facilitate comparisons across multiple different pathways and to identify key summary statistics, such as median, mean, and interquartile range. The Kolmogorov–Smirnov test was employed to test if storms in the examined pathways have statistically significant distinct latitude, longitude, sea surface temperature, and vertical shear distributions from those from all other storms in that basin. The Kolmogorov–Smirnov test is designed to identify difference in distributions rather than simply difference in means. This is done by measuring the supremum of the set of distances between the cumulative distribution functions of the two samples. The p-values were calculated, and the significance level was set to .05. If the p-value of a Kolmogorov–Smirnov test was less than .05, the distributions were labelled as significantly distinct.

3. Results

In Sections 3.1 and 3.2, we present statistics for all basins on the genesis locations and tracks of storms, stratified by genesis pathway and associated ET fractions. Based on these results, the subsequent sections focus on the North Atlantic and Western North Pacific basins.

3.1 *Genesis locations and tracks*

The tropical cyclogenesis locations for all pathways are presented in Fig. 1, defined as the location at which a storm first reaches 35-kt wind speed. There is a spatial separation between the mean development locations of storms in the baroclinic pathways LLB, STT, TI, and WTT (Table 2). The average genesis latitude of NB storms is 11.6° from the equator, whereas STT and WTT storms form on average 23.5° and 18.9° away from the equator, respectively (Table

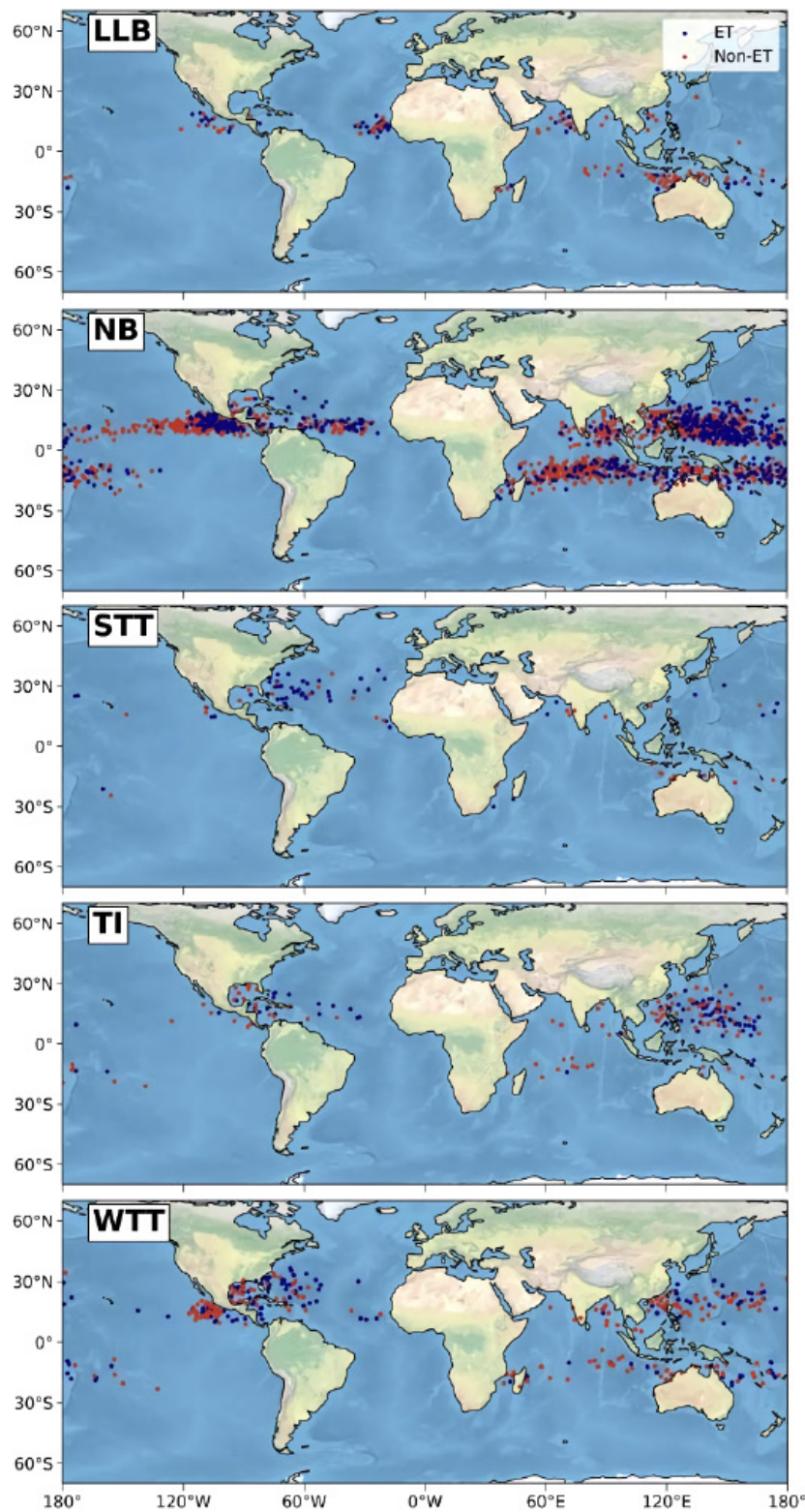


Fig. 1. Tropical cyclogenesis locations by pathway, as defined in the text, with storms labelled as ET (blue) and non-ET (red).

Table 2. Number of storms, ET fraction, and mean absolute latitude for each pathway globally.

Pathway	Number	ET fraction	Latitude
Low Level Baroclinic (LLB)	155	41.3 %	13.8°
Non-Baroclinic (NB)	1822	34.7 %	11.6°
Strong Tropical Transition (STT)	86	64.0 %	23.5°
Trough Induced (TI)	176	45.5 %	15.7°
Weak Tropical Transition (WTT)	91	40.9 %	18.9°

2). The average genesis latitude of storms in the LLB pathway is 13.8°N, and the average genesis latitude of storms in the TI pathway is 15.7°N (Table 2). When considering individual pathways, a key observation is that a majority (57.0 %) of STT storms are located in the North Atlantic. This contrasts with the TI pathway where a majority (64.2 %) of storms are located in the Western North Pacific.

Globally, storms generally form at least a few degrees away from the equator and then move poleward, reaching as high as 60°N in the Northern Hemisphere (Fig. 2). The total meridional displacements of storms that undergo ET tend to be much larger than those of non-ET storms, primarily due to rapid eastward accelerations after recurvature (Fig. 2). The latitude span of ET storm tracks also tends to be much longer than that of non-ET storm tracks (Fig. 2). In the North Atlantic, many storms follow the coastline of the United States and then recurve eastward under the influence of the midlatitude baroclinic westerlies (Kossin et al. 2010). On rare occasions, these storms even make landfall in western Europe (Sainsbury et al. 2020). Similarly, TI pathway storms in the Western North Pacific tend to move toward the northwest, with many making landfall in East Asia (Fig. 2). LLB storms are generally concentrated in the North Atlantic and Australian region basin, following a similar curvature to STT storms in the North Atlantic (Fig. 2). WTT pathway storms are concentrated in the North Atlantic and Western North Pacific. The WTT pathway contains the second-largest sample size of storms in the North Atlantic, being second only to the NB pathway (Fig. 2).

3.2 ET fractions

The number and percentage of ET and non-ET tropical cyclones were calculated by pathway for each basin (Figs. 3, 4, respectively). The global ET fraction ranges from 34.7 % to 45.5 % for storms for the LLB, NB, TI, and WTT pathways (Table 2). However, the STT pathway's global ET fraction is 64.0 % (Table 2).

This is the only pathway where a majority of storms undergo ET globally due to a high STT ET fraction (79.5 %) in the North Atlantic (Table 3). The NB, TI, and STT pathways have statistically significant distinct global ET fractions when compared with all other storms, with a confidence level greater than 95 % (Table 3).

In the North Atlantic, there are large ET fraction differences between pathways, with the LLB and STT pathways, in particular, standing out. The most striking case in the North Atlantic basin is the STT pathway where 79.5 % of storms undergo ET, statistically significant distinct from the other pathways at the 99.9 % level (Fig. 4).

The Western North Pacific basin also exhibits large differences between the ET fractions of the STT, TI, and WTT pathways and all other storms in the basin. In particular, the TI pathway has an ET fraction of 55.3 %, whereas the ET fraction of all other storms is 43.8 %, a statistically significant difference with a confidence level greater than 95 % (Fig. 4). This, combined with the large number of storms in the Western North Pacific, explains the high global ET fraction of TI storms (45.5 %).

No ET fractions of pathways in any basin other than the North Atlantic or Western North Pacific are significantly different from the others. The lack of significance for the STT pathway, in particular, in basins other than the North Atlantic is likely due to the small sample size of STT storms in other basins. The other six basins have fewer than 15 STT storms per basin. The remainder of this study focuses on the North Atlantic and Western North Pacific, as these basins contain pathways (STT and TI, respectively) with ET fractions that are statistically significantly distinct from those of the other pathways. Although the ET fractions of NB storms in the Australian, Eastern North Pacific, and North Atlantic basin are also statistically significant, the study focus was on pathways other than the NB pathway, as the NB pathway represents traditional tropical development.

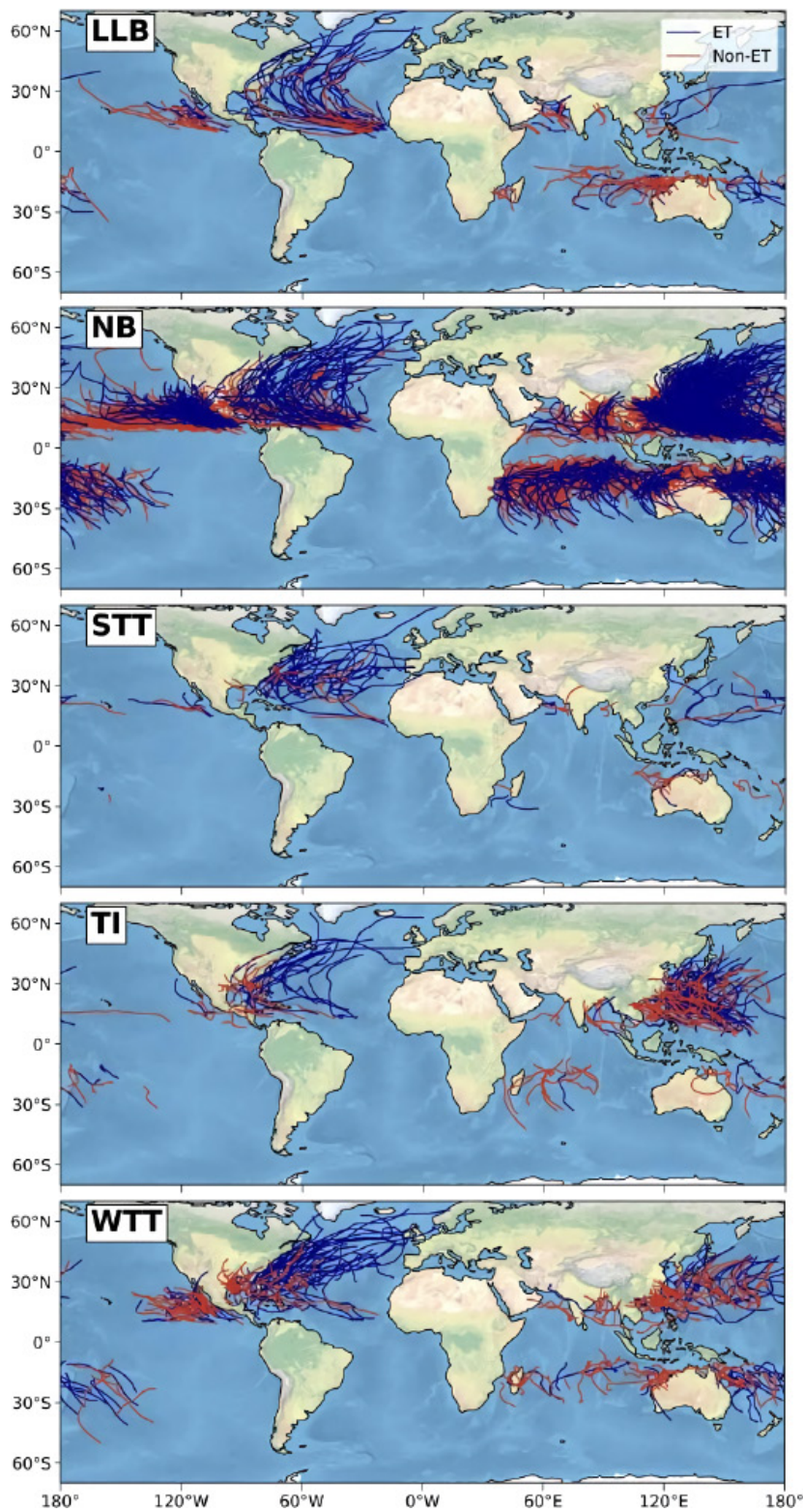


Fig. 2. Tropical cyclone tracks by pathway, as defined in the text, with storms labelled as ET (blue) or non-ET (red).

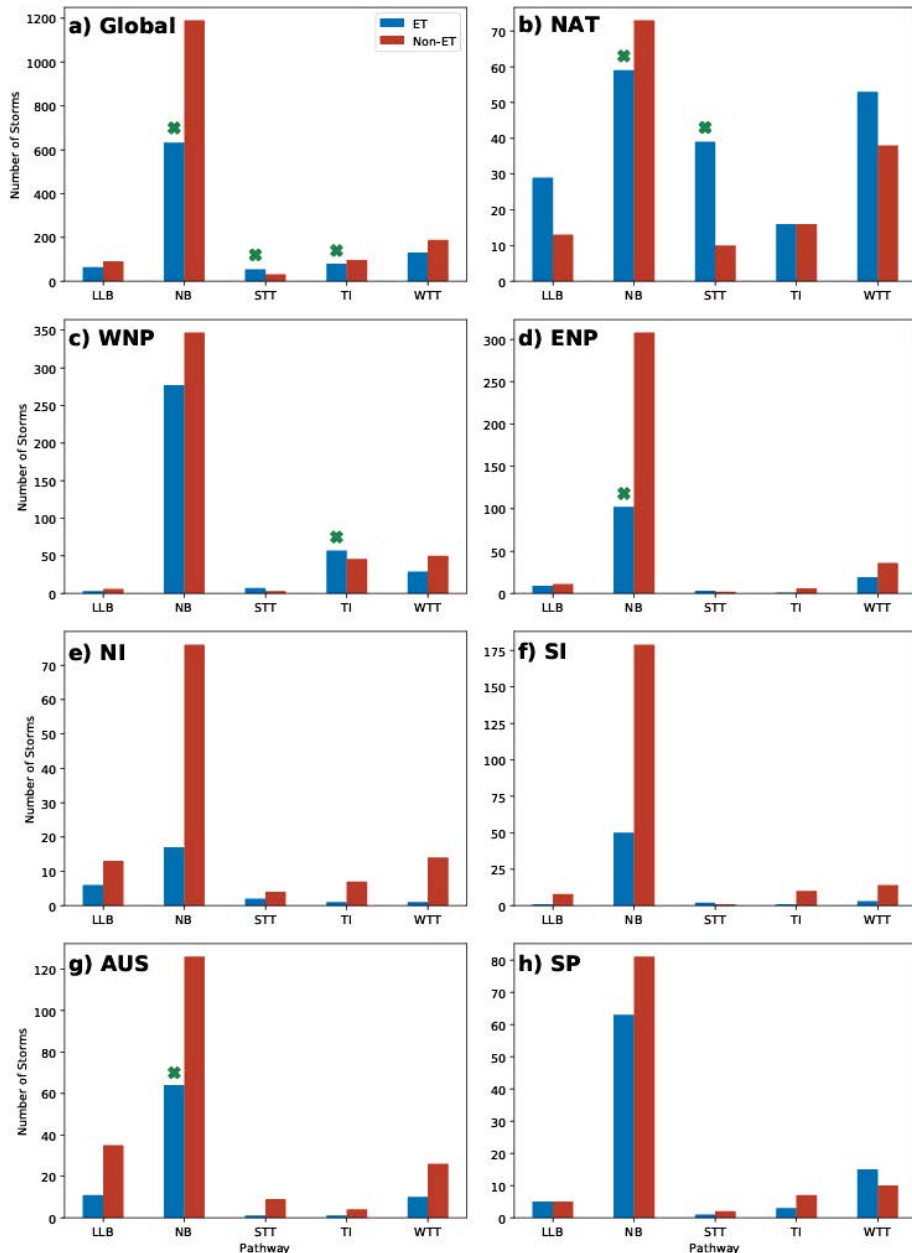


Fig. 3. Number of ET vs non-ET tropical cyclones by pathway globally and by basin. The green marker indicates a statistically significant difference in ET fraction, with a confidence level greater than 95 %, for the marked pathway.

3.3 Seasonality

In the North Atlantic (Fig. 5), the average number of storms occurring in a given month, per year, peaks in the months of August and September, with most storms occurring in the period of June to November. The ET fraction increases from 47.0 % to 60.0 % from June to November (Fig. 5). The STT pathway ET

fraction is 77 % in September and 86 % in October (Fig. 5).

For the Western North Pacific (Fig. 6), while there is a peak season between July and October, the TCs form year-around, with a minimum in February. The maximum number of storms occurs in August and September, similar to the the North Atlantic, but the

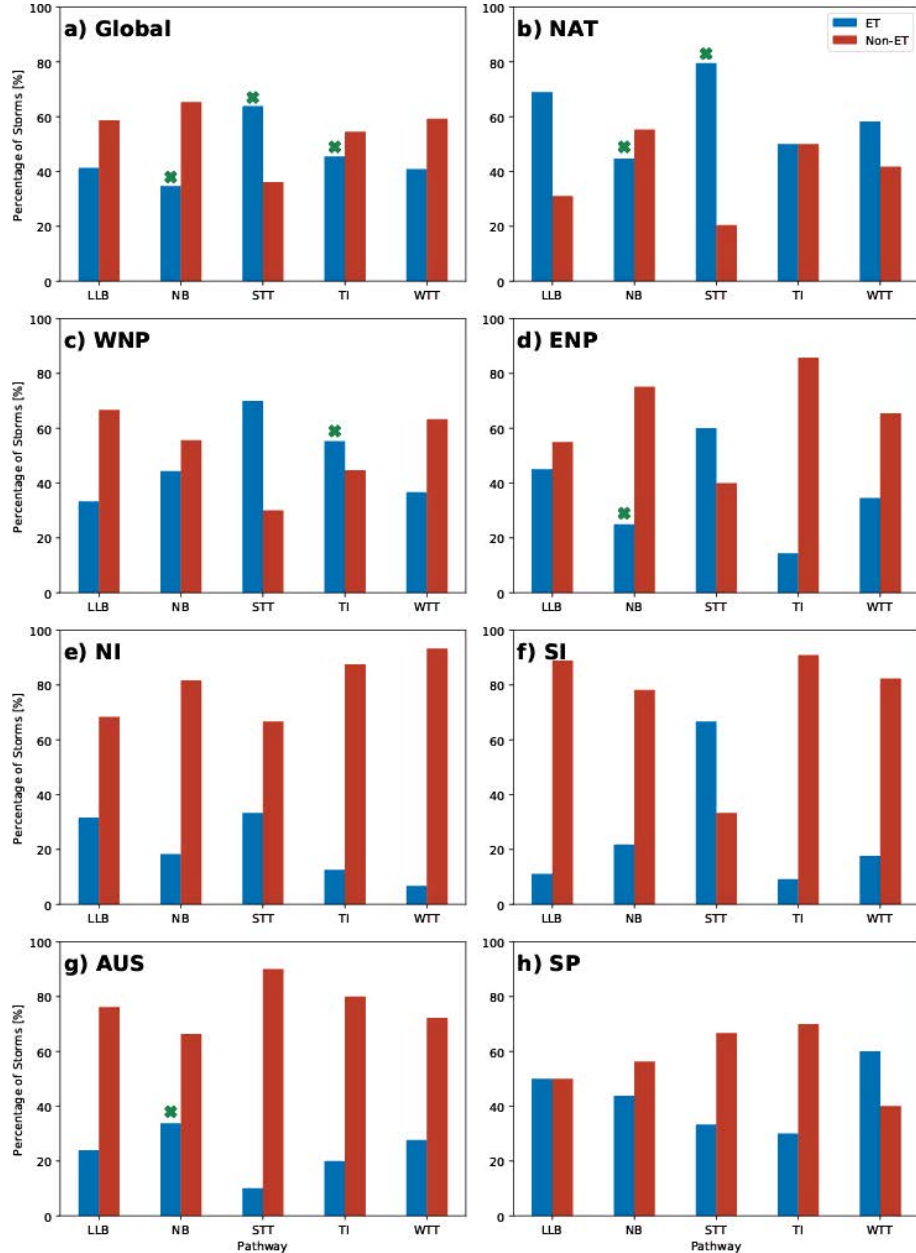


Fig. 4. Percentage of ET vs non-ET tropical cyclones by pathway globally and by basin. The green marker indicates a statistically significant difference in ET fraction for the marked pathway.

annual cycle is flatter than that of the North Atlantic (Fig. 6). This is a well-known feature of this basin as the storms are relatively more frequent in the months before and after the peak season than in the case of the North Atlantic (see, e.g., Camargo et al. 2007). The ET fraction of all storms in the Western North Pacific fluctuates between 40.0 % and 55.0 % (Fig. 6).

The ET fraction of TI storms ranges from 48.0 % to 63.0 % during the months of June to October (Fig. 6).

3.4 Environmental parameters

To better understand why ET fractions were higher for the STT and TI pathways in the North Atlantic and the Western North Pacific, the relationship between

Table 3. Number of storms, ET fraction, confidence level, and pathway globally and per basin. The confidence level in each case determines if the ET fraction for that pathway is statistically significantly different from the ET fraction of all other storms globally (or in that basin) using a Monte Carlo simulation.

Basin	Pathway	Number	ET [%]	Other storms ET [%]	Significance
Global	NB	1822	34.7 %	43.2 %	Y
Global	STT	86	64.0 %	36.6 %	Y
Global	TI	176	45.5 %	36.9 %	Y
AUS	NB	190	33.6 %	26.9 %	Y
ENP	NB	410	24.8 %	39.0 %	Y
NAT	NB	132	44.7 %	62.8 %	Y
NAT	STT	49	79.5 %	53.0 %	Y
WNP	TI	103	55.3 %	43.8 %	Y

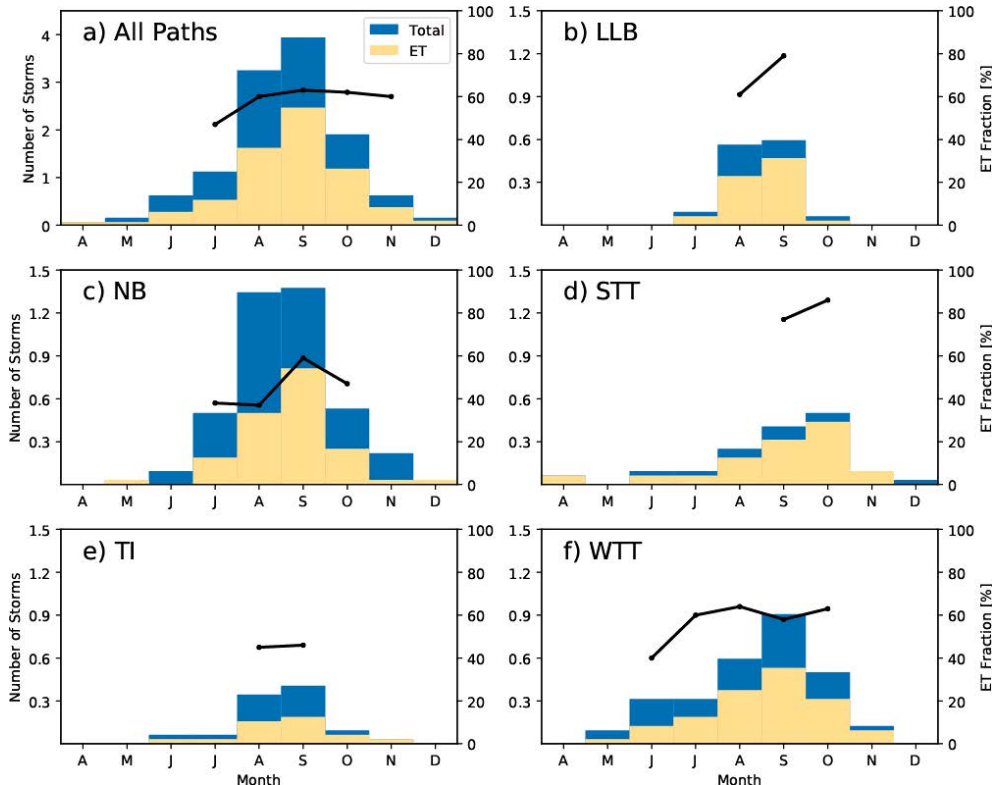


Fig. 5. Mean number of North Atlantic TCs per month: (a) all pathways, (b)–(f) by pathway. Blue bars indicate the mean number of TCs, and beige bars denote the mean number of ET storms. The black line is the ET fraction and is only shown if the total number of storms in a given month is greater than 10 in the period examined.

environmental variables and high ET fractions was analyzed. Environmental variables were tested to determine whether the storms in these pathways have environmental conditions that are more conducive to ET. The variables were selected based on the results in the study by Bieli et al. (2019), who demonstrated

that latitude and sea surface temperature (SST) are the most important variables for the prediction of ET. We also considered longitude and vertical shear in our analysis. Longitude was considered due to the observed longitudinal structure in the seasonal climatology. For each storm, the environmental variables are

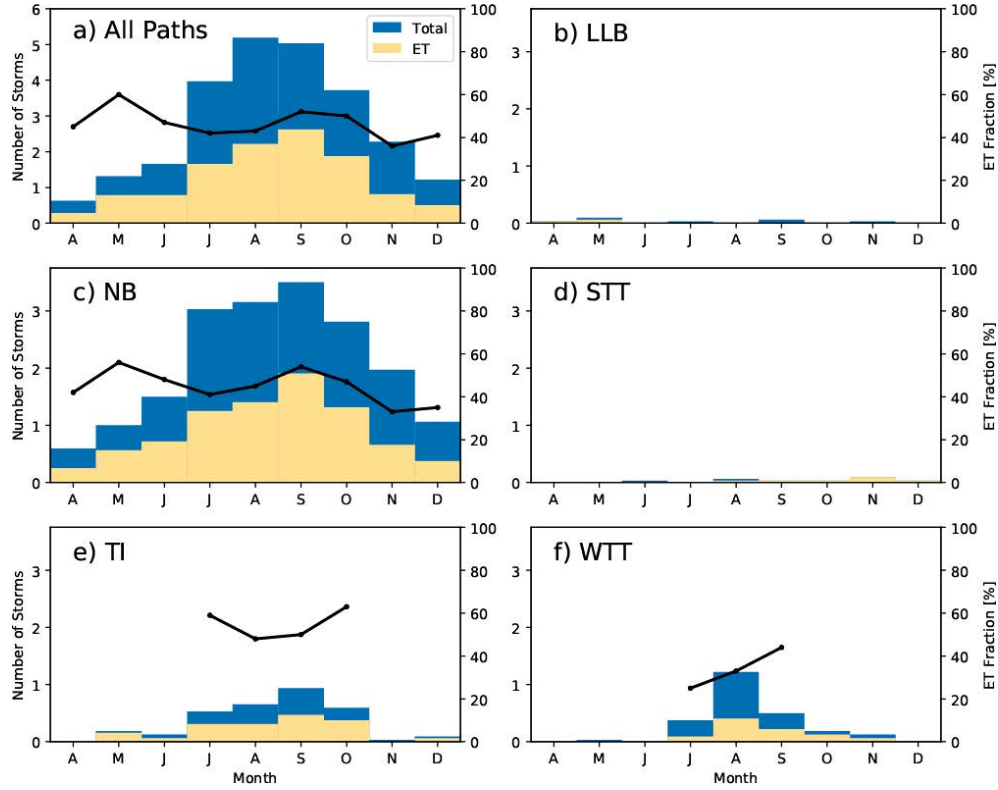


Fig. 6. Mean number of Western North Pacific TCs per month: (a) for all pathways, (b)–(f) by pathway. Blue bars indicate all TCs, and beige bars denote the mean number of ET storms. The black line is the ET fraction and is only shown if the total number of storms in a given month is greater than 10 in the period examined.

considered at the genesis location (first time in which the storm reaches a wind speed of 35 kt).

In the North Atlantic, the storms in the STT pathway have a median genesis latitude of 27.2°N, the highest median latitude value of any pathway (Fig. 7a). For instance, non-baroclinic storms have a median latitude of 13.4°N. The interquartile range of the storm latitudes for the STT pathway is 7.2° (Fig. 7a). The median genesis longitude for the STT pathway is 296°E, which lies in the center of all pathways (Fig. 7b). The median sea surface temperature of STT storms in the North Atlantic is 300.1 K, which is the lowest median sea surface temperature of any pathway in the North Atlantic (Fig. 7c). The interquartile range of the sea surface temperature for STT storms is 2.7 K (Fig. 7c). In contrast, the storms in the TI pathway have the highest median sea surface temperature at 302.1 K (Fig. 7c). The storms in the STT pathway have a median vertical shear of 10.5 m s^{-1} , which is the highest value of any pathway in the North Atlantic (Fig. 7d).

In the Western North Pacific, the median genesis latitude for TI storms is 15.6°N (Fig. 8a). TI storms have the largest latitude interquartile range of 8.5° (Fig. 8a). Although the median genesis latitude for TI storms is roughly in the middle of the different pathways, the large number of NB storms skews the latitude distribution of all other storms lower. This is further investigated in Fig. 10a, to test if the latitude distribution of TI storms is different from that of all other storms collectively in the Western North Pacific. The median genesis longitude for TI storms is 137.5°E (Fig. 8b). Most pathways have median longitudes of around 135°E (Fig. 8b). The median sea surface temperature for Western North Pacific storms in all pathways ranges from 301.9 K to 302.4 K (Fig. 8c). Additionally, the median vertical shear for the TI pathway is 7.1 m s^{-1} (Fig. 8d). This is relatively close to the values for the LLB, NB, and WTT pathways, which all have median vertical shears between 7.0 m s^{-1} and 7.8 m s^{-1} (Fig. 8d). The environmental variable distributions of TI storms were further compared

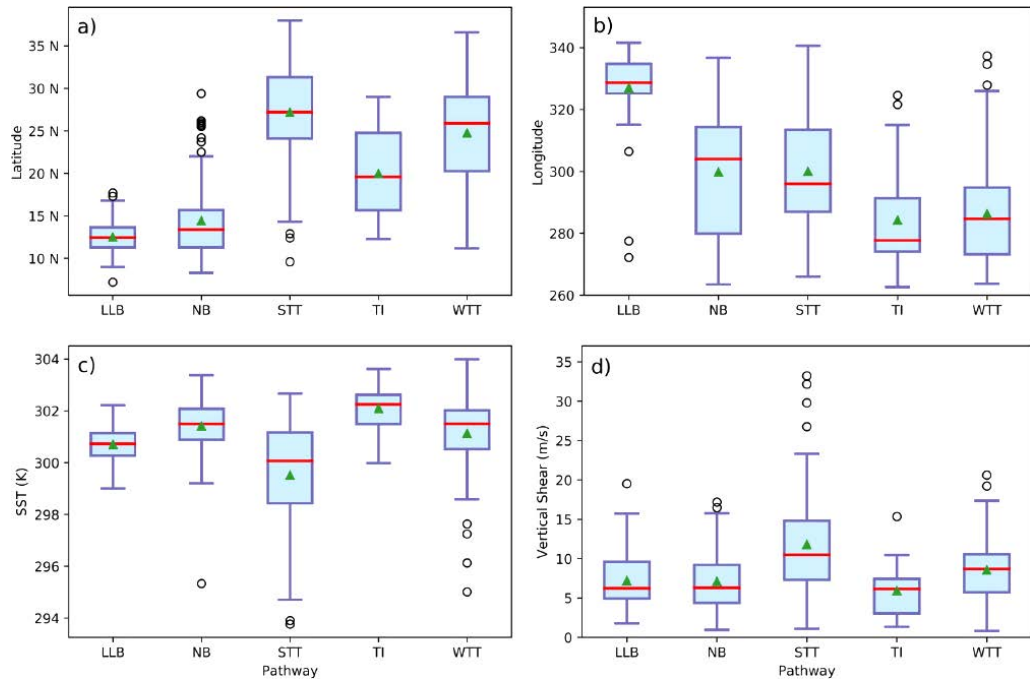


Fig. 7. Boxplots of North Atlantic TC characteristics by pathway: (a) latitude, (b) longitude, (c) SST, and (d) vertical shear. The whiskers extend to the 25th/75 percentile $\pm 1.5 \times \text{IQR}$ ($\text{Q3} - \text{Q1}$). The red line indicates the median, and the green triangle denotes the mean.

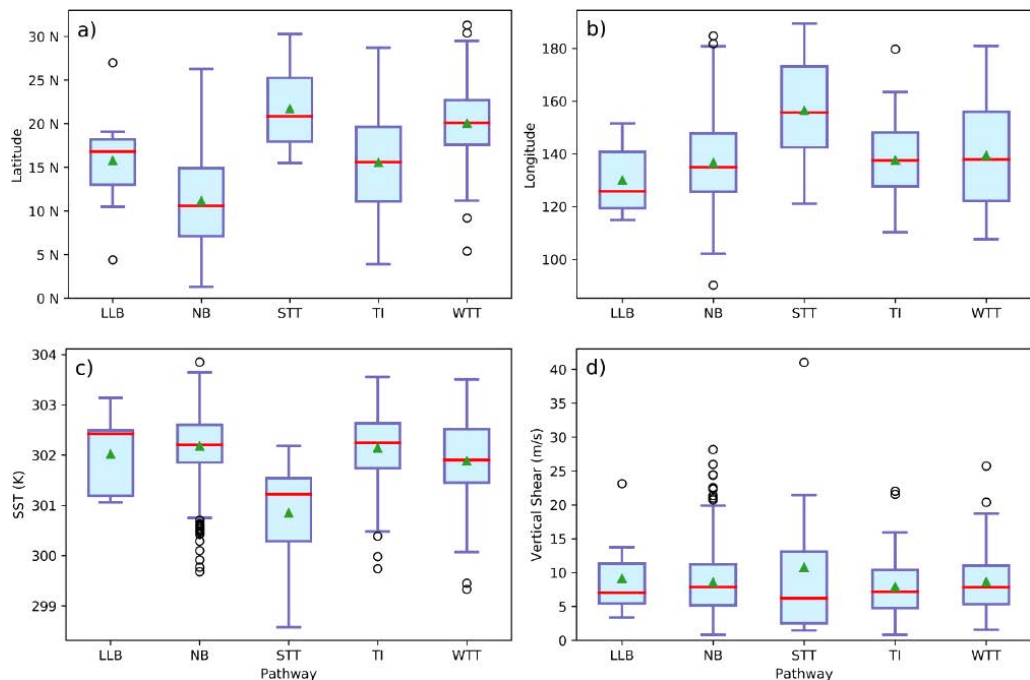


Fig. 8. Boxplots of Western North Pacific TC characteristics by pathway: (a) latitude, (b) longitude, (c) SST, and (d) vertical shear. The whiskers extend to the 25th/75th percentile $\pm 1.5 \times \text{IQR}$ ($\text{Q3} - \text{Q1}$). The red line indicates the median, and the green triangle denotes the mean.

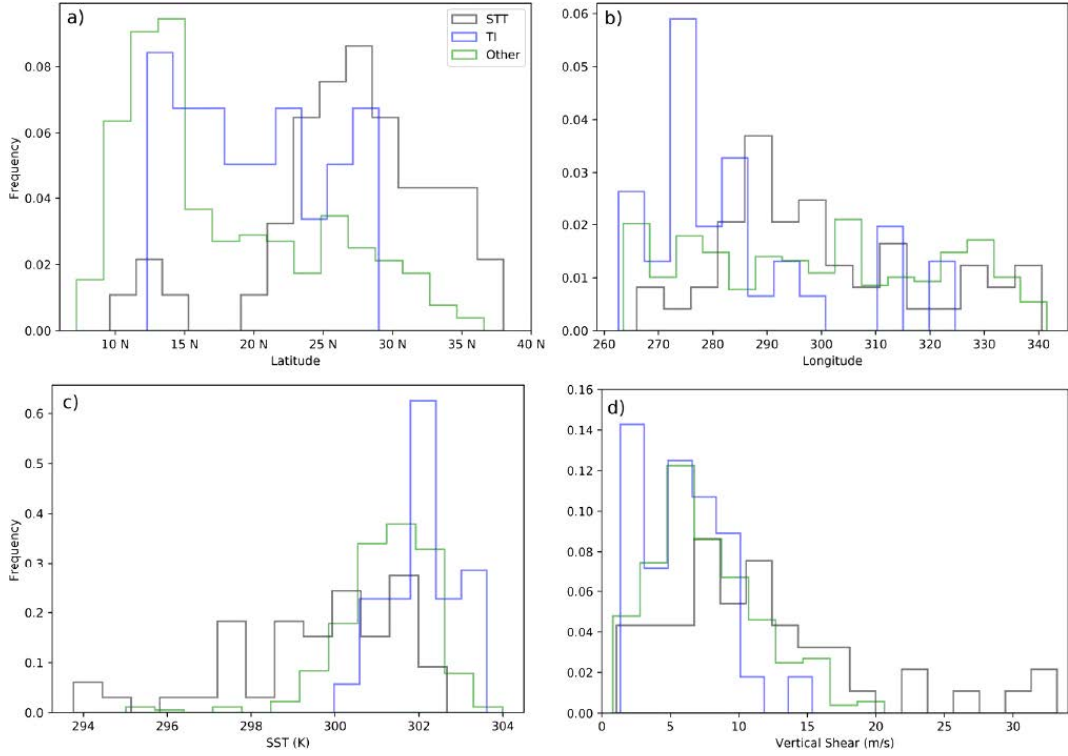


Fig. 9. Histograms of North Atlantic TCs: (a) latitude, (b) longitude, (c) SST, and (d) vertical shear in different pathways: gray denotes STT; blue, TI; and green, all other pathways.

with the collective non-TI storm distributions to better account for variations in the sample size between pathways. This analysis was conducted in Fig. 10.

In the North Atlantic, the distributions of environmental parameters of STT and TI storms were compared with those of all other pathways (Fig. 9). The distribution of genesis latitude for STT storms is skewed toward higher values, with most of the storm genesis latitudes between 22°N and 35°N (Fig. 9a). In contrast, the latitude distribution for all other storms in the North Atlantic is heavily skewed toward lower latitudes, with ranges between 10°N and 17°N (Fig. 9a). This difference in latitude distributions is statistically significant (Table 4). There is no statistically significant difference between the longitude distribution of the STT pathway compared with all other pathways. However, there is a statistically significant difference in the longitude distribution of storms in the TI pathway compared with all other cases. The vertical shear distribution for STT storms is the only distribution that contains storms with a vertical shear greater than 21 m s^{-1} (Fig. 9d). In the North Atlantic, latitude, sea surface temperature, and vertical shear

Table 4. Environmental parameters (latitude, longitude, SST, and vertical shear) by pathway globally and by basin, and if they are statistically significantly different from all storms in that case determined using the Kolmogorov-Smirnov test with a p-value of .05.

Parameter	Basin	Pathway	Significance
Latitude	NAT	STT	Y
Latitude	NAT	TI	Y
Latitude	WNP	TI	Y
Longitude	NAT	STT	N
Longitude	NAT	TI	Y
Longitude	WNP	TI	N
SST	NAT	STT	Y
SST	NAT	TI	Y
SST	WNP	TI	N
Vertical Shear	NAT	STT	Y
Vertical Shear	NAT	TI	N
Vertical Shear	WNP	TI	N

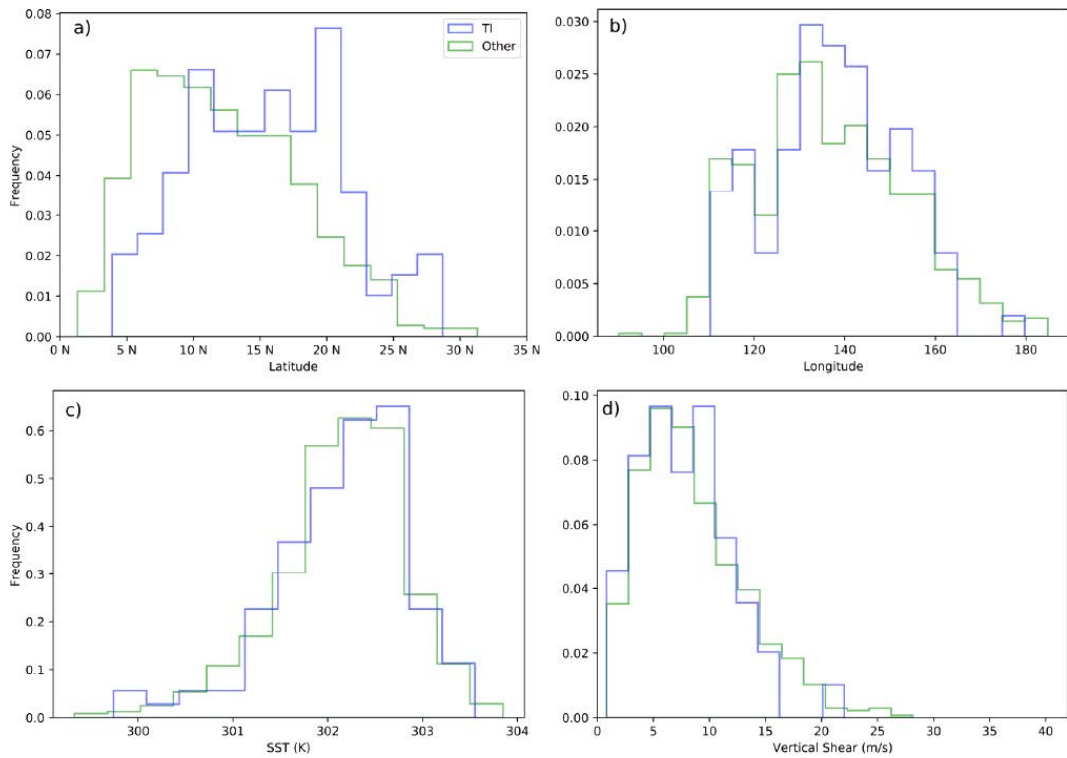


Fig. 10. Histograms of Western North Pacific TCs: (a) latitude, (b) longitude, (c) SST, and (d) vertical shear in different pathways: gray indicates STT; blue, TI; and green, all other pathways.

distributions are all distinct for the STT pathway.

In the Western North Pacific, the distributions of environmental parameters of TI storms were compared with those of all other storms (Fig. 10). The STT storm distribution was not compared with the distribution of all other storms due to a low sample size of STT storms in that basin. The latitude distribution of TI storms is roughly normally distributed about 16°N, whereas the latitude distribution of all other storms is skewed toward lower latitude values (Fig. 10a). The difference in distributions is more evident in Fig. 10a than in Fig. 8a, as the collective distribution of storms better represents the differences in sample sizes between pathways. This difference in distributions is statistically significant (Table 4). The distributions of longitude, sea surface temperature, and vertical shear for TI storms and all other storms are not statistically different (Table 4).

In examining the relationship between the latitude and longitude of STT storms in the North Atlantic, there is a visible cluster of storms in the upper region of the scatter plot in Fig. 11a, indicating that STT storms cluster around higher latitudes. Similarly, the

relationship between latitude and sea surface temperature also has a cluster in the upper middle area of the scatter plot, demonstrating that high-latitude STT storms have lower sea surface temperatures than storms in other pathways (Fig. 11b). The latitude and vertical shear scatter plot indicates a tendency for STT storms to have both higher latitudes and higher vertical shear (Fig. 11c).

In the Western North Pacific, there do not seem to be any significant clusters, when looking at multiple variables, for TI or STT storms. (Fig. 12). The relationship between latitude and longitude, latitude and sea surface temperature, and latitude and vertical shear is very similar for TI storms compared with all other storms (Fig. 12). Although the latitude distribution alone is significantly different for TI storms in the WNP, the other tested environmental variables do not exhibit environmental differences for TI storms. This result is different from the North Atlantic, where many parameters are distinct from other pathways.

Because latitude distributions were shown to be statistically significantly distinct between STT and non-STT storms in the North Atlantic, and between

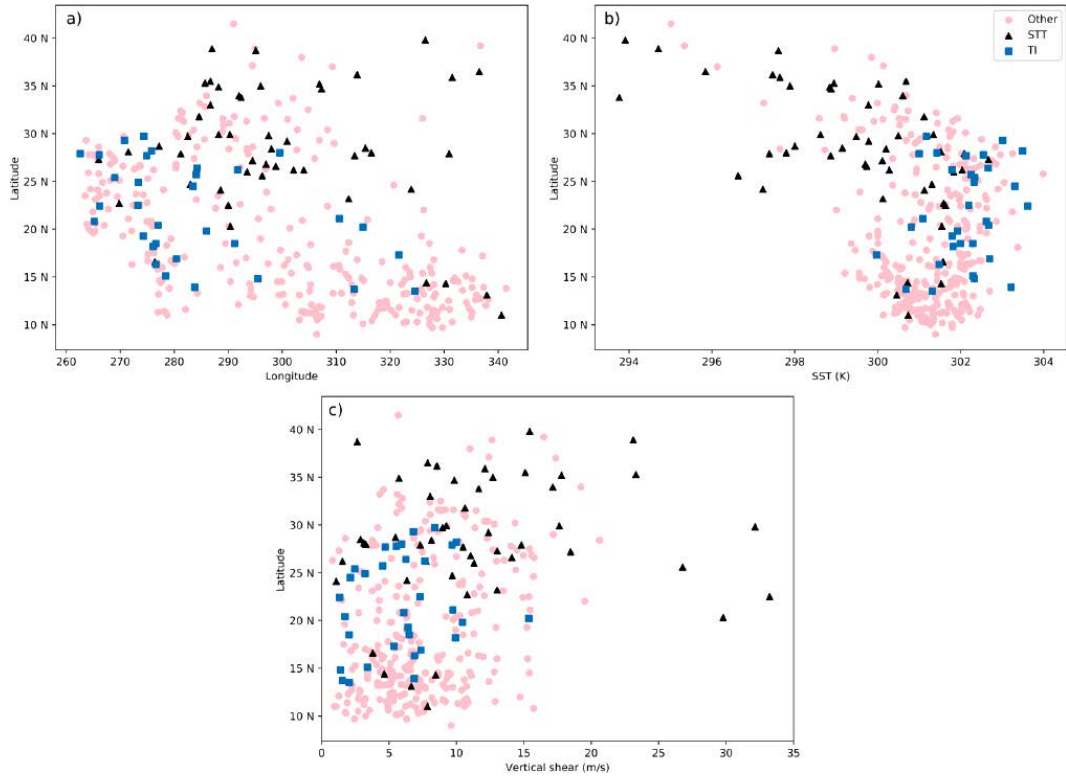


Fig. 11. Scatter plots of North Atlantic TCs comparing (a) latitude vs longitude, (b) latitude vs SST, and (c) latitude vs vertical shear for different pathways: STT are shown in black triangles, TI in blue squares, and all other pathways in pink circles.

TI and non-TI storms in the Western North Pacific, further analysis was conducted to control for latitude effects (Tables 5, 6). To eliminate latitude effects, our prior statistical analysis comparing ET fractions was conditioned on latitude bands. In the North Atlantic and Western North Pacific, storms were separated by latitude into 5° bands. A statistical test was conducted only if the number of storms in a given latitude band was greater than 10. In the North Atlantic, the STT ET fraction was compared with the non-STT ET fraction in each latitude band. The difference in ET fractions was determined to be statistically significantly different in the $20\text{--}25^{\circ}\text{N}$ and the $25\text{--}30^{\circ}\text{N}$ latitude bands (Table 5), where there is a higher number of TI storms. In the Western North Pacific, the TI ET fraction was compared with the non-TI ET fraction in each latitude band. The difference in ET fractions was determined to be statistically significantly distinct in the $10\text{--}15^{\circ}\text{N}$ and the $15\text{--}20^{\circ}\text{N}$ latitude bands (Table 6).

This result indicates that with no statistical difference between distributions of longitude, sea surface

temperature, vertical shear parameters, and a control for latitude, the ET fraction is still statistically significantly distinct in the TI pathway. This particular set of storms is quite interesting due to the lack of distinguishability by any tested factor other than pathway. Including this information should therefore improve the skill of any predictive statistical model of ET likelihood in the basin.

4. Conclusions

This paper investigates whether the physical pathway by which a tropical cyclone forms has any impact on its probability of undergoing ET later in its life. There are some pathways with statistically significant differences from other pathways when analyzing storms globally and in the Western North Pacific and North Atlantic basins, the two basins containing the most ET storms. The ET fraction of strong tropical transition (STT) storms in the North Atlantic is statistically significantly higher than the ET fraction of all other storms in the North Atlantic. In the Western

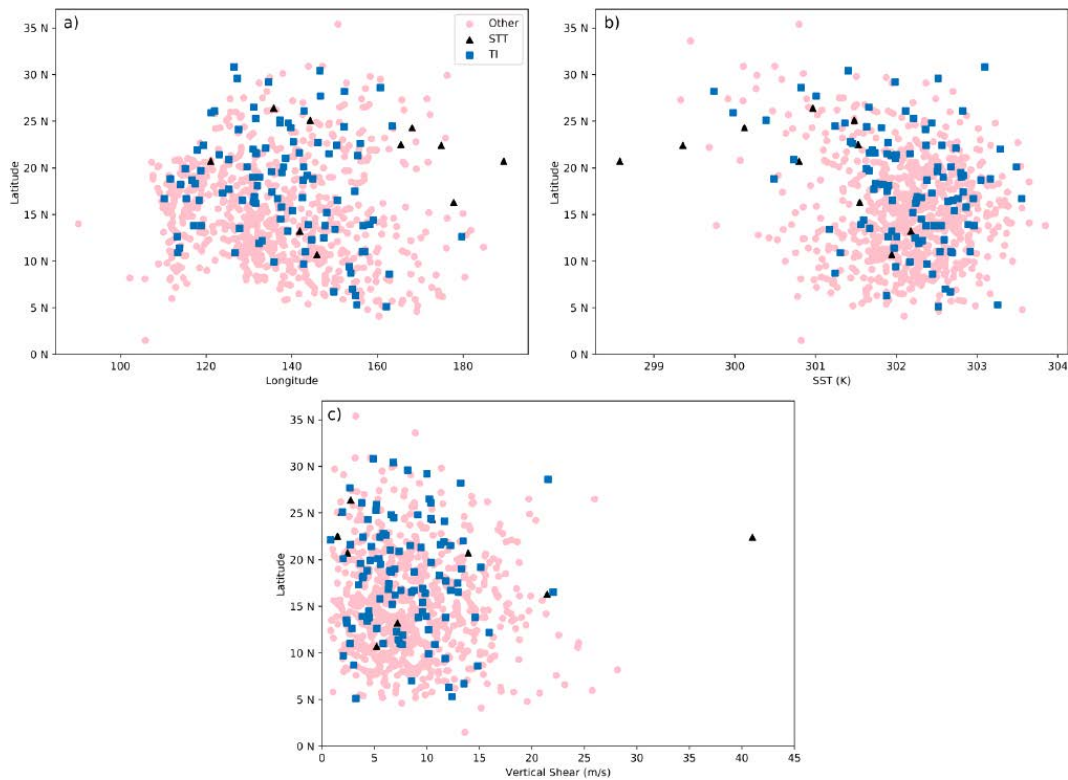


Fig. 12. Scatter plots of Western North Pacific TCs comparing (a) latitude vs longitude, (b) latitude vs SST, and (c) latitude vs vertical shear for different pathways: STT are shown in black triangles, TI in blue squares, and all other pathways in pink circles.

Table 5. Conditional latitude analysis: STT ET fraction and non-STT ET fraction by latitude band in the North Atlantic. Statistical significance of the difference in ET fraction between STT and non-STT storms is noted for sample sizes greater than 10 storms.

Basin	Pathway	Latitude band	Number of STT storms	STT ET [%]	Non-STT ET [%]	Significance
NAT	STT	< 20°N	4	50.0 %	49.5 %	
NAT	STT	20–25°N	10	80.0 %	47.4 %	Y
NAT	STT	25–30°N	25	80.0 %	56.0 %	Y
NAT	STT	30–35°N	11	90.9 %	72.0 %	N
NAT	STT	> 35°N	4	75.0 %	100.0 %	

Table 6. Conditional latitude analysis: TI ET fraction and non-TI ET fraction by latitude band in the Western North Pacific. Statistical significance of the difference in ET fraction between TI and non-TI storms is noted for sample sizes greater than 10 storms.

Basin	Pathway	Latitude band	Number of TI storms	TI ET [%]	Non-TI ET [%]	Significance
WNP	TI	0°–5°N	3	66.6 %	46.3 %	
WNP	TI	5–10°N	15	60.0 %	45.1 %	N
WNP	TI	10–15°N	31	61.2 %	43.4 %	Y
WNP	TI	15–20°N	30	53.3 %	35.7 %	Y
WNP	TI	20–25°N	18	50.0 %	50.7 %	N
WNP	TI	> 25°N	6	33.3 %	70.6 %	

North Pacific, the ET fraction of trough-induced (TI) storms is statistically significantly higher than the ET fraction of all other storms in that basin.

By controlling for formation latitude, we have demonstrated that the explanation for this relationship does not reduce to the trivial observation that TCs originating closer to the midlatitudes are more likely to interact with the baroclinic westerlies. In the North Atlantic, differences in the STT storm development environment may have a long-lasting effect on TC structure, thereby preconditioning the storm for subsequent ET. An analysis of environmental parameter and storm structural evolution would be required to determine if this is the case.

In the Western North Pacific, the lack of distinguishing environmental parameters for TI storms is equally interesting. The eastward-moving tropical upper tropospheric troughs that typically establish these TC development environments have little direct relationship with the westerly troughs associated with ET. Despite this clear separation, TCs that follow this development pathway are more likely to undergo ET. The structures and processes within the system that are responsible for such an apparent “memory” have not been identified. Future investigations of pathway-specific composite storm structural evolution might help determine the mechanisms involved.

The non-trivial relationship between storm formation pathway and ET implies a level of intrinsic predictability in the life cycle of baroclinically influenced TCs whose source is still unclear. Investigation of this source has the potential to enhance our understanding of TC-environment interactions and the persistence of information within the system. Once identified, such information could be exploited to increase the practical predictability of ET. Such an enhancement in forecast skill could be of benefit to the broad range of weather and climate studies investigating complex TC life cycles.

Data Availability Statement

The ERA-Interim reanalysis is available at <https://www.ecmwf.int/en/forecasts/datasets/reanalysis-datasets/era-interim>. The best-track datasets from the National Hurricane Center are available at <https://www.nhc.noaa.gov/data/>. The Joint-Typhoon Warning Center best-track datasets are available at <https://www.metoc.navy.mil/jtvc/jtvc.html>. The new global dataset generated and analyzed in this study, combining the best-track datasets and labels from the studies by McTaggart-Cowan et al. (2013) and Bieli et al (2019), is available at Columbia University Academic

Commons (<https://academiccommons.columbia.edu/doi/10.7916/vpx-tx12>, Datt et al. 2022).

Acknowledgments

SJC and AHS acknowledge support from NASA grant 80NSSC17K0196, under the NASA Modeling, Analysis, and Prediction program. We also acknowledge the Vetslesen Foundation for their generous and sustained support of climate science at the Lamont-Doherty Earth Observatory.

References

- Bentley, A. M., and N. D. Metz, 2016: Tropical transition of an unnamed, high-latitude, tropical cyclone over the eastern North Pacific. *Mon. Wea. Rev.*, **144**, 713–736.
- Bieli, M., S. J. Camargo, A. H. Sobel, J. L. Evans, and T. Hall, 2019: A global climatology of extratropical transition. Part I: Characteristics across basins. *J. Climate*, **32**, 3557–3582.
- Bieli, M., A. H. Sobel, S. J. Camargo, and M. K. Tippett, 2020: A statistical model to predict the extratropical transition of tropical cyclones. *Wea. Forecasting*, **35**, 451–466.
- Camargo, S. J., A. W. Robertson, S. J. Gaffney, P. Smyth, and M. Ghil, 2007: Cluster analysis of typhoon tracks. Part I: General properties. *J. Climate*, **20**, 3635–3653.
- Datt, I., S. J. Camargo, A. H. Sobel, R. McTaggart-Cowan, and Z. Wang, 2022: *Data: An investigation of tropical cyclone development pathways as an indicator of extratropical transition*. Columbia Academic Commons, doi:10.7916/vpx-tx12.
- Davis, C. A., and L. F. Bosart, 2003: Baroclinically induced tropical cyclogenesis. *Mon. Wea. Rev.*, **131**, 2730–2747.
- Davis, C. A., and L. F. Bosart, 2004: The TT problem: Forecasting the tropical transition of cyclones. *Bull. Amer. Meteor. Soc.*, **85**, 1657–1662.
- Dee, D. P., S. M. Uppala, A. J. Simmons, P. Berrisford, P. Poli, S. Kobayashi, U. Andrae, M. A. Balmaseda, G. Balsamo, P. Bauer, P. Bechtold, A. C. M. Beljaars, L. van de Berg, J. Bidlot, N. Bormann, C. Delsol, R. Dragani, M. Fuentes, A. J. Geer, L. Haimberger, S. B. Healy, H. Hersbach, E. V. Hólm, L. Isaksen, P. Källberg, M. Köhler, M. Matricardi, A. P. McNally, B. M. Monge-Sanz, J.-J. Morcrette, B.-K. Park, C. Peubey, P. de Rosnay, C. Tavolato, J.-N. Thépaut, and F. Vitart, 2011: The ERA-Interim reanalysis: Configuration and performance of the data assimilation system. *Quart. J. Roy. Meteor. Soc.*, **137**, 553–597.
- Emanuel, K., 2018: 100 years of progress in tropical cyclone research. *Meteor. Monogr.*, **15**, 15.1–15.68.
- Evans, C., K. M. Wood, S. D. Aberson, H. M. Archambault, S. M. Milrad, L. F. Bosart, K. L. Corbosiero, C. A. Davis, J. R. D. Pinto, J. Doyle, C. Fogarty, T. J. Galarneau, Jr., C. M. Grams, K. S. Griffin, J. Gyakum, R.

- E. Hart, N. Kitabatake, H. S. Lentink, R. McTaggart-Cowan, W. Perrie, J. F. D. Quinting, C. A. Reynolds, M. Riemer, E. A. Ritchie, Y. Sun, and F. Zhang, 2017: The extratropical transition of tropical cyclones. Part I: Cyclone evolution and direct impacts. *Mon. Wea. Rev.*, **145**, 4317–4344.
- Fudeyasu, H., and R. Yoshida, 2018: Western North Pacific tropical cyclone characteristics stratified by genesis environment. *Mon. Wea. Rev.*, **146**, 435–446.
- Galarneau, T. J., Jr., C. A. Davis, and M. A. Shapiro, 2013: Intensification of Hurricane Sandy (2012) through extratropical warm core seclusion. *Mon. Wea. Rev.*, **141**, 4296–4321.
- Hart, R. E., 2003: A cyclone phase space derived from thermal wind and thermal asymmetry. *Mon. Wea. Rev.*, **131**, 585–616.
- Jones, S. C., P. A. Harr, J. Abraham, L. F. Bosart, P. J. Bowyer, J. L. Evans, D. E. Hanley, B. N. Hanstrum, R. E. Hart, F. Lalaurette, M. R. Sinclair, R. K. Smith, and C. Thorncroft, 2003: The extratropical transition of tropical cyclones: Forecast challenges, current understanding, and future directions. *Wea. Forecasting*, **18**, 1052–1092.
- Keller, J. H., C. M. Grams, M. Riemer, H. M. Archambault, L. Bosart, J. D. Doyle, J. L. Evans, T. J. Galarneau, Jr., K. Griffin, P. A. Harr, N. Kitabatake, R. McTaggart-Cowan, F. Pantillon, J. F. Quinting, C. A. Reynolds, E. A. Ritchie, R. D. Torn, and F. Zhang, 2019: The extratropical transition of tropical cyclones. Part II: Interaction with the midlatitude flow, downstream impacts, and implications for predictability. *Mon. Wea. Rev.*, **147**, 1077–1106.
- Kossin, J. P., S. J. Camargo, and M. Sitkowski, 2010: Climate modulation of North Atlantic hurricane tracks. *J. Climate*, **23**, 3057–3076.
- Mauk, R. G., and J. S. Hobgood, 2012: Tropical cyclone formation in environments with cool SST and high wind shear over the northeastern Atlantic Ocean. *Wea. Forecasting*, **27**, 1433–1448.
- McTaggart-Cowan, R., G. D. Deane, L. F. Bosart, C. A. Davis, and T. J. Galarneau, Jr., 2008: Climatology of tropical cyclogenesis in the North Atlantic (1948–2004). *Mon. Wea. Rev.*, **136**, 1284–1304.
- McTaggart-Cowan, R., T. J. Galarneau, Jr., L. F. Bosart, R. W. Moore, and O. Martius, 2013: A global climatology of baroclinically influenced tropical cyclogenesis. *Mon. Wea. Rev.*, **141**, 1963–1989.
- Sainsbury, E. M., R. K. H. Schiemann, K. I. Hodges, L. C. Shaffrey, A. J. Baker, and K. T. Bhatia, 2020: How important are post-tropical cyclones for European windstorm risks? *Geophys. Res. Lett.*, **47**, e2020GL089853, doi:10.1029/2020GL089853.
- Tang, B. H., J. Fang, A. Bentley, G. Kilroy, M. Nakano, M.-S. Park, V. P. M. Rajasree, Z. Wang, A. A. Wing, and L. Wu, 2020: Recent advances in research on tropical cyclogenesis. *Trop. Cyclone Res. Rev.*, **9**, 87–105.